Density-matrix renormalization-group method for excited states

M. Chandross and J. C. Hicks
SPAWAR Systems Center, Code D364, San Diego, California 92152
(Received 21 October 1998)

The density-matrix renormalization-group (DMRG) method can provide approximate ground-state wave functions for many one-dimensional systems with a high degree of accuracy. Conventional DMRG techniques, however, cannot be expected to give accurate excited-state information because the excited states of interest are not explicitly included in the calculations. We discuss techniques for extending DMRG to accurately target and investigate arbitrary excited states. As an example we apply the method to investigate the properties of excitons within the extended Hubbard model. Our results show that excited-state calculations within the standard DMRG procedure give results that are quantitatively incorrect. [S0163-1829(99)11715-6]

I. INTRODUCTION

The density-matrix renormalization-group (DMRG) method, introduced by White,[1] has proven to be extremely successful for calculating the ground-state properties of model Hamiltonians for very large system sizes in one dimension.[1–6] While conventional DMRG is designed purely to target the ground state of a given system at zero temperature only, a number of extensions to the method have been developed. For example, the ''symmetrized DMRG'' method is a useful tool for probing the lowest-energy wave functions in multiple symmetry subspaces,[3–6] while the transfer-matrix DMRG method[7] has been developed as a method for calculating thermodynamic properties such as specific heat or magnetization of lattice systems. The use of DMRG to probe higher energy excited states, however, is a relatively recent development.[6] We point out here that because conventional DMRG only targets the ground-state wave function, serious errors in both the energies and wave functions for excited states can result from a calculation in which the specific excited states are not targeted.

We present here a simple procedure that can effectively target arbitrary excited states of model Hamiltonians within the DMRG procedure. In Sec. II we briefly discuss the general DMRG method and point out why it is only suited for ground-state calculations. We then introduce our method for extracting excited-state information in Sec. III. In Sec. IV we discuss the application of our method to the identification of excitons within the extended Hubbard model.

II. GROUND-STATE DMRG

In the DMRG method,[1] a system of a given size, referred to as a superblock, is divided into two pieces, the system block and the environment block. The reduced probability density matrix for the system block is formed from an eigenstate of the superblock $|\psi\rangle$,

$$\rho_{ii'} = \sum_j \psi_{ij}\psi_{i'j} \tag{1}$$

where the superblock wave function has been written as $|\psi\rangle = \Sigma_{ij}\psi_{ij}|i\rangle|j\rangle$, with $|i\rangle$ and $|j\rangle$ representing the basis states of the system block and the environment block, respectively. The eigenstates of $\rho_{ii'}$ with the largest eigenvalues then represent the most probable configurations of the system block, given that the superblock is in the eigenstate $|\psi\rangle$. In the conventional DMRG algorithm $|\psi\rangle$ is the ground-state wave function $|\psi_{\mathrm{GS}}\rangle$. When the eigenstates corresponding to the smaller eigenvalues of $\rho_{ii'}$ are discarded, the truncated basis represents the dominant configurations for the *ground state* of the superblock. For small system sizes, a subset of these configurations will undoubtedly reasonably represent excited states of the superblock. However, as the system size is increased, the excited state information will gradually be pruned away.

III. EXCITED-STATE DMRG

In order to extract excited-state information from the DMRG procedure, it is necessary to retain information about the relevant excited states of the superblock. As the ground state is the only state that can be identified by an eigenvalue alone, it is crucial to be able to identify the desired excited states by their eigenvectors.

As as example, we briefly introduce here the method we use in Sec. IV to study excitons within the extended Hubbard Hamiltonian. It has previously been shown in the ''essential states'' method of nonlinear optics[8] that it is possible to identify the threshold of the electron-hole continuum though three successive applications of the dipole operator. We begin by finding the ground state (and a number of even-parity excited states) with a standard Lançzos procedure. We then find an odd-parity vector ψ_μ by applying the dipole operator to the ground state and normalizing the resulting vector. We use ψ_μ as the initial Lançzos vector for a second Lançzos procedure aimed at retrieving a number of odd-parity eigenstates. The odd-parity eigenstate that has the largest dipole matrix element with ψ_{GS} is identified as the $1B_u$. The largest dipole matrix element of the $1B_u$ with the even-parity eigenstates from the initial Lançzos procedure identifies the mA_g, where m is a quantum number that depends on parameters and system size. Similarly, the largest dipole matrix element between the mA_g and the odd-parity eigenstates identifies the nB_u, with n again a quantum number dependent on system size and parameters. The mA_g and nB_u have been identified

as an even-parity exciton and the threshold of the conduction band, respectively, in exact calculations on small systems,[8,9] but their true long-chain nature is still unclear.

Information from the eigenstates identified above can be included in the reduced probability density matrix $\rho_{ii'}$ through two methods. The first method assumes that the superblock is simply a mixed state of the relevant wave functions. We do not use this method in order to avoid possible phase cancellations which may arise from the straight addition of the wave functions. Rather, we add probability densities by first forming a reduced probability density matrix $\rho_{ii'}$ for each of the above eigenstates, and then construct a final density matrix for the superblock from an equally weighted linear combination of the individual matrices.

IV. SAMPLE APPLICATION

We now demonstrate the importance of this simple procedure in a calculation within the extended-Hubbard model, a qualitative model for conjugated polymers. The procedure for other model Hamiltonians is similar, with the major difference being the choice of an appropriate operator which picks out the eigenstates of interest. We write the Hamiltonian as

$$H=-t\sum_{i\sigma}\,[1-(-1)^i\delta](c^{\dagger}_{i\sigma}c_{i+1\sigma}+c^{\dagger}_{i+1\sigma}c_{i\sigma}) + \sum_{i}\,[Un_{i\uparrow}n_{i\downarrow}+V(n_i-1)(n_{i+1}-1)], \qquad (2)$$

where $c^{\dagger}_{i\sigma}$ creates an electron of spin σ on site i, $n_{i\sigma}$ is the number of electrons of spin σ on site i, and $n_i=\Sigma_\sigma n_{i\sigma}$. The system is given a static dimerization through the bond alternation parameter δ which modifies the nearest-neighbor electron hopping term t. U and V describe the on-site and nearest-neighbor electron-electron interactions, respectively. We consider the half-filled band only.

We begin by comparing our results with a conventional DMRG calculation with $U=3t$, $V=t$, and $\delta=0.1$ in order to demonstrate the importance of targeting excited states. Additionally, we will be making comparisons with conventional DMRG calculations performed by other groups.[3,6] While our results indicate that the $1B_u$ is an exciton for our parameters, previous work has found that this state is unbound. In Ref. 3, the authors find a negative gap between the $1B_u$ and the calculated charge gap, and conclude that there are no excitons. We believe that the charge gap is only relevant in a quasiparticle formulation and does not represent the energy of the continuum in a true many-body calculation. The authors of Ref. 6 find the continuum via the essential states method, and then examine the behavior of an approximate ''average particle-hole separation'' as a function of system size to conclude that the $1B_u$ is unbound. While we believe that this quantity is too approximate to be an accurate method of separating bound and unbound excitations, we feel that the major shortcoming of this work is from not targeting all relevant excited states. We now show the errors incurred by such a calculation.

In Fig. 1(a) we plot the excitation energies of the $1B_u$, mA_g, and nB_u (Ref. 10) as a function of system size using

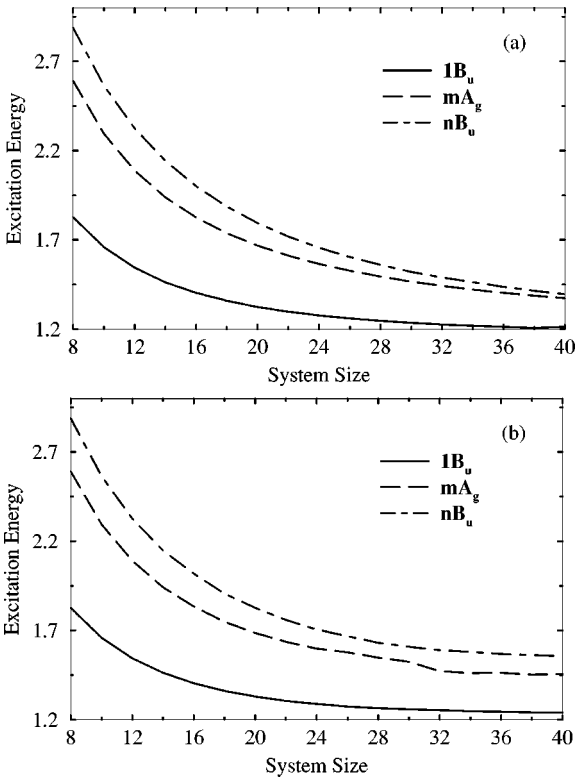

FIG. 1. Excitation energies of the $1B_u$, mA_g, and nB_u for $U=3t$, $V=t$, and $\delta=0.1$ as a function of chain length with the reduced probability density matrix representing (a) all four states and (b) only the ground state.

the method outlined above for $U=3t$, $V=t$, and $\delta=0.1$, the values typically used for polyacetylene. In comparison we show in Fig. 1(b) the same plot with only the ground-state information retained. In all calculations we keep 250 states in the DMRG truncation procedure. While the curves are relatively smooth in both cases (the minor variations in the curves can be improved by keeping more states in the truncation procedure and performing more iterations in the Lanczos diagonalization), the excitation energies are substantially different in the long-chain limit. As expected, the energies of the $1A_g$ ground state and the $1B_u$ are reasonably correct (within $\simeq 3\%$) in the conventional DMRG procedure. However, both the mA_g and nB_u states in Fig. 1(b) lie above the nB_u state in Fig. 1(a). Further inaccuracies are seen in the density-density correlation function at each state s,

$$f^j_s(i)=\langle (n_i-1)(n_{i+j}-1)\rangle_s \qquad (3)$$

for all sites i. In Figs. 2(a) and 2(b) we compare $f^0_s(i)$ [relative to $f^0_{1A_g}(i)$] for the $1B_u$, mA_g, and nB_u for our method and conventional DMRG, respectively, for 36 sites. For the half-filled band, this is equivalent to $2\langle n_{i,\uparrow}n_{i,\downarrow}\rangle_s$, which tracks the location of double occupancies. Figure 2(a) indicates that the double occupancies in the $1B_u$ favor the center of the chain, whereas the correlation functions of the mA_g and nB_u are more spatially delocalized, with lower occupancies at the chain center. The correlation functions in Fig. 2(b) are very different from those in Fig. 2(a). The similarities for the $1B_u$ are not surprising, as the $1B_u$ has the lowest eigenvalue in the B_u subspace. However, the correlation functions

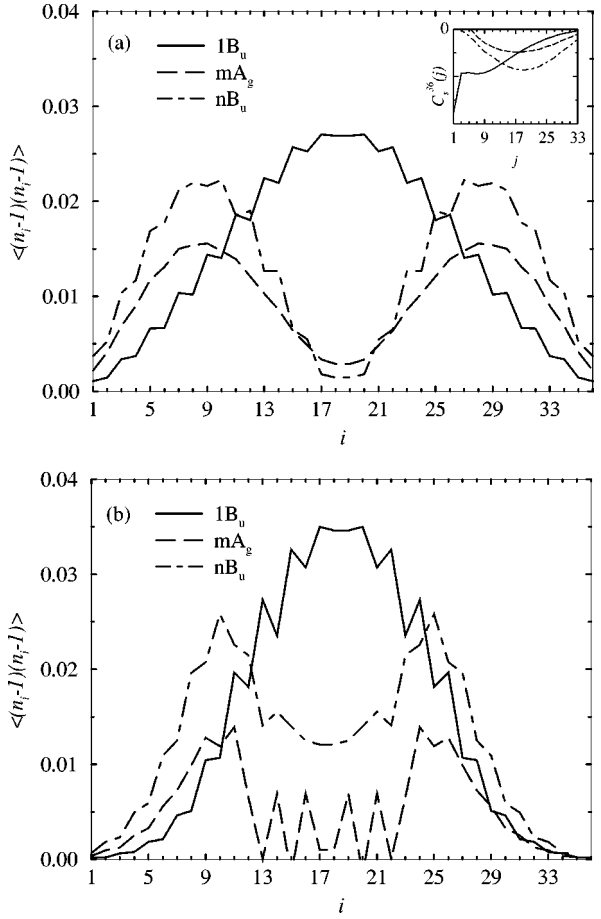

FIG. 2. The correlation function $f_s^0(i)$ for $s = 1B_u$, mA_g, and nB_u with $U=3t$, $V=t$, and $\delta=0.1$ and the reduced probability density matrix representing (a) all four states and (b) only the ground state. The inset in (a) shows $C_s^N(j)$; see text.

of the mA_g and nB_u, while exhibiting some of the same qualitative features, give grossly incorrect quantitative results. In particular, the mA_g in Fig. 2(b) shows rapid oscillations near the chain center where Fig. 2(a) shows a smoothly varying function.

We now proceed to the demonstration of binding in the $1B_u$ through an analysis of both the energies and wave functions of the essential states found above. From this point forward, we will only discuss the results of DMRG calculations in which all relevant excited states are targeted.

From an energetic standpoint, we first note that in Fig. 1(a) there is an indication of a finite gap between the $1B_u$ and the nB_u in the long-chain limit. We have extrapolated the energies of the essential states with a polynomial fit[11] and found that the gap will persist in long chains. In models that do not support excitons (i.e., without intersite Coulomb interactions), the mA_g and the two states to which it is most strongly dipole-coupled become degenerate as the chain length increases. The lack of such convergence in Fig. 1(a) and in the extrapolated eigenvalues[11] indicates that the $1B_u$ is an exciton.

We begin our examination of the wave functions by first returning to Fig. 2(a). The correlation functions in Fig. 2(a) clearly show that the $1B_u$ and the mA_g and nB_u belong to different classes of wave functions; the $1B_u$ is spatially localized near the chain center, already indicating excitonic

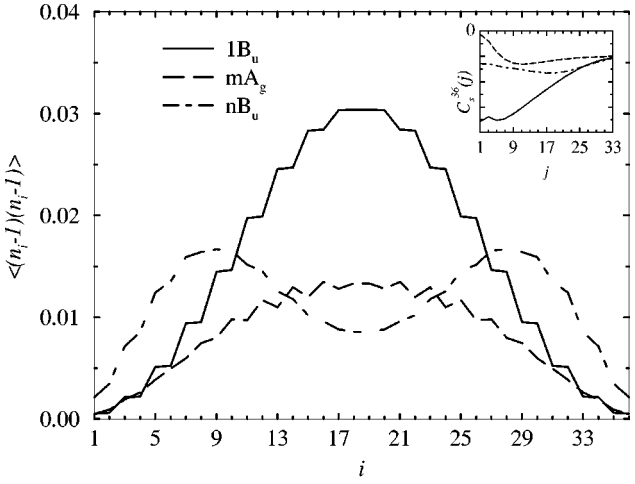

FIG. 3. The correlation function $f_s^0(i)$ for $s = 1B_u$, mA_g, and nB_u with $U=3t$, $V=t$, and $\delta=0.3$. The correlation functions are nearly identical for $\delta=0.5$. Note that for large δ, the $f_{mA_g}^0(i)$ becomes closer to $f_{1B_u}^0(i)$. The inset shows $C_s^N(j)$; see text.

character. On the other hand, the double occupancies in the mA_g and nB_u tend to be found more in the outer thirds of the chain. This alone, however, does not indicate continuum character as the possibility exists that these eigenstates are excitonic with the electron-hole pair residing in the outer portions of the chain.

To resolve this issue, we turn to the centered correlation function defined in Ref. 6,

$$C_s^N(j)=\frac{1}{2}\left[f_s^j\left(\frac{N-j+1}{2}\right)+f_s^j\left(\frac{N-j-1}{2}\right)\right], \qquad (4)$$

where the averaging is performed to account for the differing bond lengths when $\delta>0$. As in Ref. 6, we only consider odd distance (i.e., negative) contributions. Although $C_s^N(j)$ only uses two different values of i for each j (rather than averaging over the entire chain), and cannot quantitatively represent the true correlation, it can still be used in a qualitative fashion to determine whether the electron and hole in a given wave function are correlated over short or long distances. To this end, we do not sum over different values of j, as in Ref. 6, but rather plot $C_s^N(j)$ *as a function of* j.

In the inset of Fig. 2(a) we show $C_s^{36}(j)$ for the $1B_u$, mA_g, and nB_u. The plot of $C_{1B_u}^{36}(j)$ indicates that the electrons and holes $1B_u$ are strongly (weakly) correlated at short (large) distances. This again demonstrates the excitonic character of the $1B_u$. In contrast, $C_{mA_g}^{36}(j)$ and $C_{nB_u}^{36}(j)$ show that the strongest correlation in these states occurs near $j=19$, precisely the distance between the two peaks in $f_s^0(i)$. We thus conclude that these are continuum states. We believe that Fig. 2(a) is the *first realization* of the nature of the correlated conduction band.

With increasing bond alternation, the extended-Hubbard model can be used to describe different conjugated polymers. In Fig. 3 we show $f_s^0(i)$ for the essential states with $U=3t$, $V=t$, and $\delta=0.3$, parameters typically used for the polysilanes. The shapes of $f_{1B_u}^0(i)$ and $f_{nB_u}^0(i)$ are virtually

unchanged by the value of δ, being characterized by one and two peaks, respectively. The same one- and two-peak spectra are found for $f^0_{1B_u}(i)$ and $f^0_{nB_u}(i)$, respectively, with $\delta=0.5$, as well as in the more strongly correlated case of $U=5t$ and $V=2t$ (Ref. 11) (we note that for the latter parameters, both Refs. 3 and 13 classify the $1B_u$ as a bound state[12]). On the other hand, as the dimerization increases, the shape of $f^0_{mA_g}(i)$ shifts from two peaks at $\delta=0.1$ to one peak at $\delta=0.3$ and 0.5. The long-range correlation functions, shown in the inset of Fig. 3, indicate that the assignments for the essential states remain the same as for $\delta=0.1$, namely the $1B_u$ is an exciton, and the mA_g and nB_u are continuum states. Our results cannot give a definitive answer as to which state, the mA_g or the nB_u, is the continuum threshold in the long-chain limit. The classification of the mA_g as the continuum threshold by the authors of Ref. 6 is consistent with Fig. 1(a), in which the mA_g is lower in energy than the nB_u. However, our extrapolations for large system sizes indicate that the eigenvalues cross at very large system sizes ($\sim$80 sites),[11] and the nB_u becomes the continuum threshold, as it is traditionally defined.[8] As the accuracy of extrapolated eigenvalues is always highly questionable, however, we simply note that the indication that the energies of the mA_g and nB_u at least converge in the long-chain limit further reinforces their classification as continuum states.

V. CONCLUSION

The DMRG method can be used effectively to investigate excited-state properties, as long as information regarding the states of interest is included in the reduced probability density matrix. We have outlined a simple procedure for targeting arbitrary excited states provided they can be identified at all system sizes. Our application to excitons within the extended Hubbard model demonstrates both the ease of the method as well as the potential for serious error when excited states are not properly targeted. We have demonstrated that for $U=3t$, $V=t$ with various values of δ, the $1B_u$ is an exciton, and the mA_g and nB_u are continuum states. The interesting question of the classification of the mA_g for stronger Coulomb interactions and long-range interactions remains. We note that, at least for $\delta=0.3$ and 0.5, the extended Hubbard model does seem to support more than one exciton state. For both these parameter sets, we find a distinct B_u state below the mA_g that is similar to the hydrogenic $2S$ state. The correlation function $f^0_s(j)$ shows a three-peak spectrum, which can be classified through $C^N_s(j)$ as a strongly bound electron-hole pair at the chain center coexisting with a continuumlike pair in the outer areas of the chain.

ACKNOWLEDGMENTS

We would like to thank Professor S.R. White at U.C. Irvine for useful discussions. This research was funded through the Independent Research program at SPAWAR Systems Center, San Diego. We would also like to acknowledge the assistance of the NRC.

[1] S. R. White, Phys. Rev. Lett. **69**, 2863 (1992); Phys. Rev. B **48**, 10 345 (1993).
[2] H. B. Pang and S. D. Liang, Phys. Rev. B **51**, 10 287 (1995).
[3] Z. Shuai, S. K. Pati, W. P. Su, J. L. Brédas, and S. Ramasesha, Phys. Rev. B **55**, 15 368 (1997).
[4] M. Boman, R. J. Bursill, and W. Barford, Synth. Met. **85**, 1059 (1997).
[5] S. Ramasesha, S. K. Pati, H. R. Krishnamurthy, Z. Shuai, and J. L. Brédas, Synth. Met. **85**, 1019 (1997).
[6] M. Boman and R. J. Bursill, Phys. Rev. B **57**, 15 167 (1998).
[7] T. Nishino, J. Phys. Soc. Jpn. **64**, L3598 (1995); R. J. Bursil, T. Xiang, and G. A. Gehring, J. Phys.: Condens. Matter **8**, L583 (1996); X. Wang and T. Xiang, cond-mat 970531 (unpublished).
[8] D. Guo, S. Mazumdar, S. N. Dixit, F. Kajzar, F. Jarka, Y. Kawabe, and N. Peyghambarian, Phys. Rev. B **48**, 1433 (1993).
[9] M. Chandross, Y. Shimoi, and S. Mazumdar, Chem. Phys. Lett. **280**, 85 (1997); Phys. Rev. B (to be published).
[10] In short chains we find that, as in Ref. 6, two B_u states have large dipole couplings to the mA_g. By nB_u here, we refer to the state that evolves into the long-chain nB_u.
[11] M. Chandross and J. C. Hicks (unpublished).
[12] Additionally, a recent study of the extended-Hubbard Hamiltonian in the $U\rightarrow\infty$ limit has also found that bound states exist for $V\geqslant 2t$ only with any value of U (Ref. 13).
[13] F. B. Gallagher and S. Mazumdar, Phys. Rev. B **56**, 15 025 (1997).